Journal of ELECTRICAL ENGINEERING, VOL. 56, NO. 11-12, 2005, 313–321

RIPPLE CONTROL SIGNAL USING FOR EARTH FAULT LOCATION IN MV NETWORKS

Petr Toman — Jaroslava Orságová *

At present, digital protections using the admittance principle are able to identify quite reliably a single phase-to-ground connection and to determine the affected feeder. Still, the location of the fault presents a task yet to be solved. The main problem of a fault location consists is a low value of the fault current during a single phase-to-ground fault in compensated networks. This work started of an experiment performed in the second half of 2001. The experiment explored the possibility of identifying the fault location in a circular network by means of ripple-control signal. The work deals with a novel method for fault location that is able to determine the distance of a fault in a radial network (without possibility of circular interconnection) using only values measured in a switching station. The principle of this method was published in 2000 [1]. It presents the application of the method in a real distribution network and the evaluation of the results of this experiment.

K e y w o r d s: single phase-to-earth faults, compensated network, location of faults, ripple-control signal

1 EARTH FAULT LOCATION IN CIRCLE NETWORK

A connection between a phase conductor and the ground in MV networks is called an earth fault. Since the fault current in this case does not depend on the point of the fault, but only on the total capacity (size) of a network, the earth fault location keeps being a problem for MV network operators. This paper describes an experiment carried out in a MV network in order to verify the functionality of a method for earth fault location in a ringed network.

1.1 Introduction

The experiment was based on the theory worked out by the Haefely-Trench company that was modified by using ripple control signal injection. Sections of the line (Fig. 1.1) marked ***a*** and ***b*** represent a MV line with an earth fault, section ***c*** represents a line that is ringed with the affected line and section ***d*** represents the rest of the non-affected part of the network. According to the calculations performed in the Matlab 5.2 program, the point of earth fault in a ringed network depends on the zero-sequence current ratio according to Fig. 1.2 (a line with AlFe 95 mm^2 conductors was used).

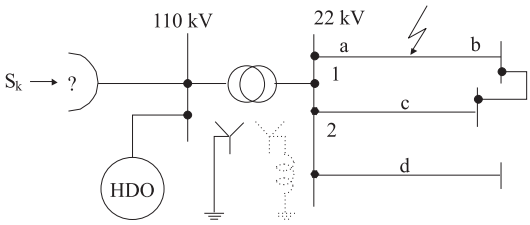

Fig. 1.1. Elementary diagram of the method.

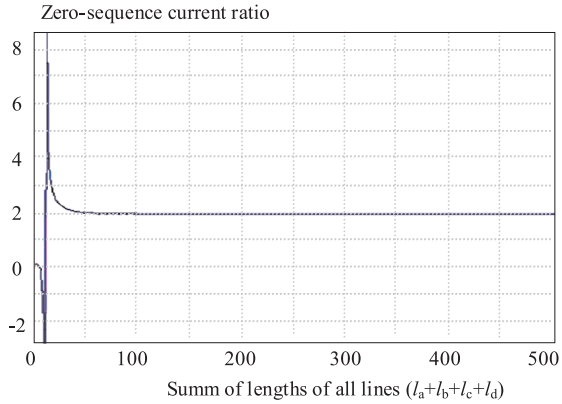

Fig. 1.2. Zero-sequence current ratio I_{01}/I_{02}, ringed lines impedance $Z_a/(Z_b + Z_c) = 0.5$, ringed lines length 30 km; l_a = 10 km, l_b = 10 km, l_c = 10 km.

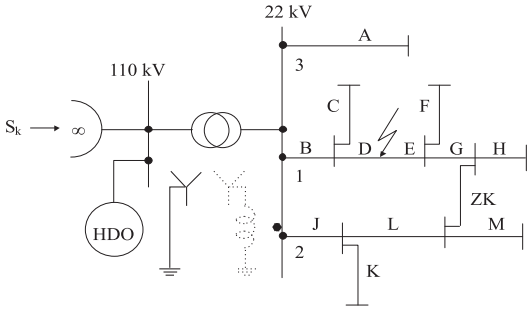

Fig. 1.3. Simplified network scheme during measuring.

1.2 Measuring

Measuring was performed during normal operation, with a fault simulated on a loaded line. Measuring was made in two steps. First, after earth fault, the affected and non- affected lines were ringed. Then a ripple control signal was injected into 110 kV network.

* Department of Electrical Power Engineering, Faculty of Electrical Engineering and Communication of Brno University of Technology, Technická 2848/8, 616 00 Brno, Czech Republic, E-mail: toman@feec.vutbr.cz

ISSN 1335-3632

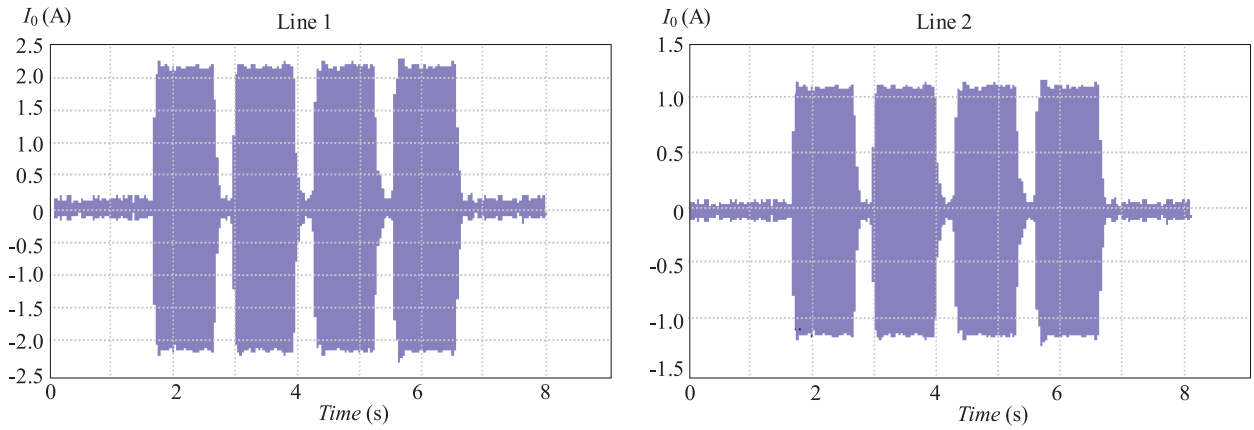

Fig. 1.4. Zero-sequence currents in the lines.

Table 1.1. Line parameters for ripple control signal frequency

Parameter	Line 1 Length B+D	Line 2 Length E+G+J+L	Ratio Line 1/ Line 2	Ratio Line 2/ Line 1
$R_{0.216}\,(\Omega)$	10.28	22.32	0.461	2.17
$X_{0.216}\,(\Omega)$	67.72	140.1	0.483	2.07
$Z_{0.216}\,(\Omega)$	68.49	141.8	0.483	2.07

Table 1.2. Zero-sequence current ratio

Ground Connection	I_0 Line 1 (A)	I_0 Line 2 (A)	I_0 Line 1 / Line 2
Metallic, 108 A	9.7	4.5	2.15
Metallic, 136 A	9.2	4.4	2.09
Conductor on the earth, 136 A	2.2	1.1	2.0
Conductor on the earth, 108 A	1.9	0.95	2.0

The experiments were performed for four types of ground connection:

a) metallic ground connection,
b) conductor fallen on the earth,
c) arc ground connection,
d) conductor fallen on a tree.

Then for each type three measurements for different capacity of the connected non-affected network were made: 21 A, 108 A, 136 A.

The automatic for connecting a resistor after earth fault was disabled.

1.3 Measured Values Analysis

The ripple control signal in the ringed lines was taken out of the measured values by means of a digital filter. The zero-sequence current ratio is approximately equal to the inverse ratio of impedances for measuring. Zero-sequence currents are nearly purely inductive (within the range of the precision of analysis $90° \pm 3°$). The following types of ground connection could be used for earth fault measuring:

– metallic ground connection
– conductor fallen on the earth

with network capacity ranges of 108 and 136 A.

In the case of network capacity range of 21 A the level of the signal transmitted to the measuring transformer output side was very small. As far as measuring for arc ground connection is concerned, it was not possible to separate the ripple control signal from the other inter-harmonics generated by the arc. In the case of ground connection caused by a conductor fallen on a tree the level of the signal transmitted to the measuring transformer output side was again very small.

The accuracy of earth fault location is relatively good for the cases where the point of fault could be located; the greatest error is ±750 meters. Thus for a loop length of about 30 km corresponds in our case for 1 % of the current ratio approximately with 100 m of line length. To express this dependence more in detail a sensitivity analysis would have to be performed because the range of error on 1 % ratio changes with the value of the ratio.

It can be concluded from the results that measuring in a ringed loop using the ripple control signal is relatively accurate and the results — providing a sufficient accuracy of measured values correspond to reality.

1.4 Using the Method of Ringing with the Frequency of Ripple Control Signal

The method of earth fault location in a ringed network can be divided in two cases:

– earth fault location using 50 Hz frequency,
– earth fault location using ripple control signal frequency of 216.66 Hz.

To sum up this analysis, it can be concluded that the method of ringing at the frequency of 50 Hz can be used if the following conditions are fulfilled:

– sufficient accuracy of measuring zero-sequence currents in ringed lines, especially their effective parts,
– the ringed lines with fault are connected to the same busbar as the non-affected network of a sufficient

length (capacity), which means at least three times greater than the length (capacity) of the ringed lines (including branches), the exact multiple depends on the character of the network,

Disadvantages:

- the current ratio for a fault close to a switching station is a big number, hence any change (inaccuracy) means a big distance (error of fault location),
- it is not always possible to ring the affected line with the non-affected one connected to the same busbar system,
- if an earth fault appears on a radial line connected to the affected line, only the distance of the point where the line is connected to the loop formed by the ringed lines can be found.

In order to eliminate the condition of locating the point of fault from the effective parts of zero-sequence currents a method of injecting an interharmonic signal into the network was proposed. Since a system of ripple control of electrical heating using an interharmonic frequency (mostly 216.66 Hz a 183.33 Hz) is available, a signal of frequency of 216.66 Hz was applied. Simplified calculations showed a decreasing dependence on the length of the connected non-affected network and thus there was no need to separate effective and reactive parts of zero-sequence currents. That is why a more precise model respecting also branches in ringed lines was created. Including branches decreased slightly the accuracy and it can be concluded that if the sum of the lengths of branches in one line increases many times the length of the loop, the accuracy of earth fault location will significantly decrease. It was also confirmed that a compensated network at the frequency of ripple control signal behaves as an isolated one.

The analysis of the ringed lines during the earth fault showed that increasing the length of the connected non-affected network causes a flow of a capacitive current in the longer line of the loop to the busbars instead of flowing to the point of the earth fault. This phenomenon is caused by greater capacitive currents of the sections of the loop and a negligible current of the compensating coil. If the length of the non-affected network increases, the capacitive current flowing to the busbars decreases until its sign changes and it starts flowing to the point of the earth fault. This can explain bouncing in current ratio calculations because the value of current in the denominator is small (for a certain length of the connected non-affected network can be equal to zero). Only if the currents from the lines in the loop are negligible in comparison with the capacitive current of the non-affected network, the accuracy of the method of earth fault location is sufficient for a practical application.

Advantages of using ripple control signal:

- the method is not affected with load,
- the network is compensated for frequency 50 Hz, it behaves as an isolated one for the frequency of ripple control signal,
- it is not necessary to separate effective and reactive parts of zero-sequence currents.

Disadvantages:

- only a signal at the frequency of ripple control signal is measured, which means that a filter must be used,
- if an earth fault appears, a switching station must ask a dispatching center of 110 kV network to send a neutral ripple control signal message that will not affect the receivers of consumers.

1.5 Conclusions

The practical application of the described method would require the installation of a computer in a 110/22 kV switching station where the whole network would be programmed including its current configuration. Zero-sequence currents from all lines are measured and then only the frequency of the ripple control signal is selected in a filter. If an earth fault appears, the program will propose a point for ringing the network. The ringing is done by the dispatcher who will also ask for sending a ripple control signal. When zero-sequence currents are measured, the loop is disconnected and the computer will calculate the zero- sequence current ratio and then the point of the earth fault. If it is necessary, the result can be checked by calculation for a given configuration. The calculation is performed by means of node analysis whose application (including the simulation of switching points) on computers is relatively easy.

It would be also necessary to perform an economical analysis of the method before its practical application. The analysis should consider the return of investment in view of introducing a competitive electricity market and increasing demands for the quality of supply.

2 EARTH FAULT LOCATION IN RADIAL NETWORK

This part presents a method for the location of a single phase-to-ground fault by means of remote control signal of frequency of 216.6 Hz. It uses a known searching algorithm that has been modified according to a verification experiment for radial distribution networks in the Czech Republic.

2.1 Experiment Description

Verification of the method for single phase-to-ground fault location was made in three phases. In the first phase, necessary parameters and data were obtained and measuring in a real 22 kV distribution network during a simulation of a ground fault was performed. Then the data were processed and applied to ground fault location. It was necessary to use a frequency different from the basic value of 50 Hz for measuring. Measuring was performed by the ripple-control signal because it is easily available in networks of this type. Measuring includes the testing of a theoretical possibility of utilization of fault recorders of digital protective devices for ground fault location.

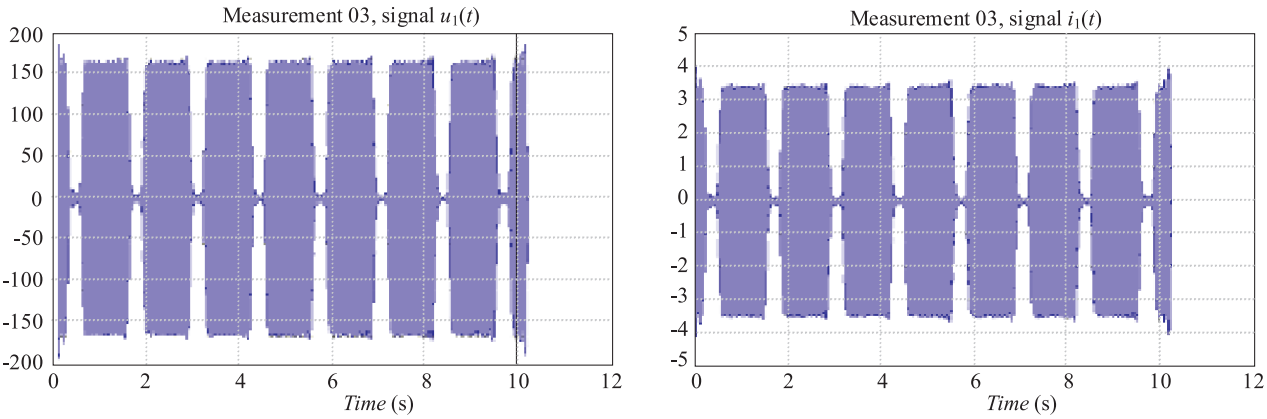

Fig. 2.1. Time responses of instantaneous voltage $u(t)$ (V) and current $i(t)$ (A) to the ripple-control signal with frequency $f = 216.6$ Hz obtained from BK 550 A during the 3rd series of measuring.

Description of the Measured Locality

The experiment was performed at the Ptáčov switching station of the JME Company near Třebíč between November 20 and 21, 2002. The single phase-to-ground fault was achieved artificially in terminal VN98, in phase L1 of a branch near the village of Číměř about 600 m from the ripple-controlled circuit breaker number 104. The line is composed mainly of an overhead line; a cable line is just between the terminal output in the station and the first tower of the line. Terminal VN98 was loaded being operated as circular one. The measuring was performed both in the short-circuiting and input sections of the 22 kV switching station (output terminal of a 110/22 kV transformer).

Each test was performed in four steps:

1. Preparation of short-circuiting section for a given type of ground fault and the change of network configuration to a required capacity range.
2. Starting a ripple-control signal transmitter.
3. Connecting the fault with circuit breaker number 104 controlled locally.
4. Switching off circuit breaker number 104 after 5–20 seconds according to type of fault

Measuring Equipment

BK 550 analyzer of networks (model DEWE 2010) was installed in the input section of the 22 kV switching station. It allows to record time responses of four currents and four voltages with a sampling frequency of 6.4 kHz. The voltage was read by means of R-C dividers with a voltage division ratio of 1 : 250 and precision 0.5 % that had been installed in the point of measuring. The voltage output module of the analyzer was DAQP-DMM, ranges 120 V and 230 V, precision 0.1 %. The currents were measured by means of AMPFLEX A100 flexible current converters with a range of 1000 A/1 V and precision 1 %. The parameters of DAQP-V input module of the analyzer were the following: range 1 V, precision 0.1 %.

The following protecting terminals were connected to the fixed converters during the measurement: REF 543 (ABB) and SEPAM 1000, model 42 (Schneider-Electric). The parameters of their fault recorders were as follows: REM 543 — sample frequency 2 kHz and maximum time of recording for 8 recorded channels 2.5 s, SEPAM 1000 — sample frequency 600 Hz and maximum time of recording for 7 recorded channels 10 s.

PRYM instrument for measuring fault current and voltage (sample frequency 7.2 kHz) produced by the EGU Brno was installed in the short-circuiting section. Voltage and current were read by means of measuring voltage and current transformers. Maximum time of recording in two channels was 40 s.

The aim of the principal part of the measuring was to get time response of at frequency of 216.66 Hz and first of all to find root mean square values and phase angles of phase voltages and currents. This task was solved by means of Matlab 6.0 software. Signal from the analyzer was modified into the form of matrix applicable in the program. Then a number of samples necessary for the fast Fourier transformation were added. After the transformation into frequency plane, a zone near the frequency of ripple-control signal with a bandwidth of 30 Hz was chosen. Then the inverse Fourier transformation back to time plane was performed. After that, signal root mean square value and phase angle were calculated.

2.2 Calculation of the Probable Distance of the Point of the Fault by Means of the Measured Values

The mathematical model of the network is composed of three transmission elements for each of the symmetrical components that represent the network between the supply and the point of the fault. Using the inverse cascade equations of the elements, the symmetrical components currents and voltages at the beginning of the tested part were found. Data obtained directly from the control system of the regional JME dispatching center were incorporated into the network model. These data represented

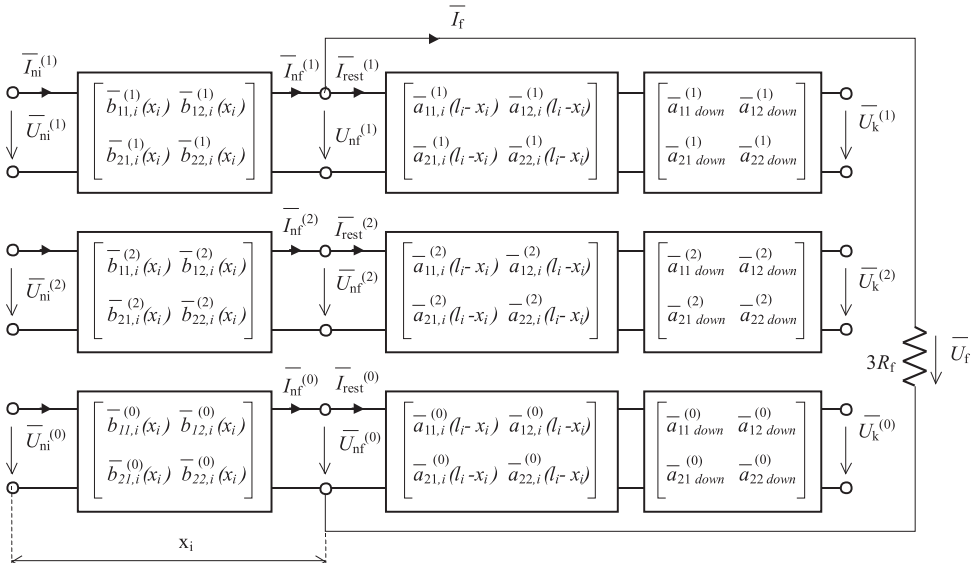

Fig. 2.2. Interconnection of transmission elements at the point of fault.

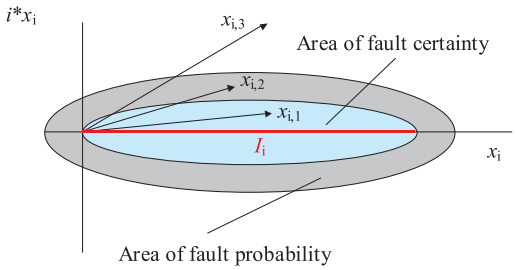

Fig. 2.3. Evaluating criterion for polynomial roots.

the topology of the whole network including the lengths of line sections and conductor parameters (type and cross section). Calculation was conducted by means of Matlab program.

Since the values of currents and voltages at ripple-control signal frequency were used during the calculation, network parameters were recalculated to this frequency by multiplying their imaginary parts by factor $k_f = f_{HDO}/f_n$.

Two variants of admittance network were set up for the purpose of calculation. One of them included load shunt admittances in corresponding buses. These admittances were calculated out of the distribution of the total network load measured at the basic frequency proportionally to individual loads. The load was supposed to be symmetrical.

The tested part was replaced by a cascade connection of two Π-equivalent circuits. The roots of the polynomial as possible values of the fault distance were calculated for all variants of measuring at resistive ground faults.

The final part of the criterial equation (and mainly its right-hand side, where current $\overline{I}_{rest}$ in the part of the network behind the point of the fault is found) has a crucial importance for the results of calculation.

The interconnection of the transmission elements of the parts of the network including the description of the coefficients of the corresponding matrices that is used as a base for forming the resulting criterial equation is shown in Fig. 2.2.

Current $\overline{I}_{rest}$ is — as well as voltages and currents at the point of the fault — a function of fault distance x_i :

$$\begin{aligned}\overline{I}_{rest}^{(1)}(l_i - x_i) &= \overline{U}_{nf}^{(1)}(x_i) \cdot \overline{y}_{rest,11}^{(1)}(l_i - x_i)\,,\\ \overline{I}_{rest}^{(1)}(l_i - x_i) &= \left(\overline{b}_{i,11}^{(1)}(x_i) \cdot \overline{U}_{in}^{(1)} + \overline{b}_{i,12}^{(1)}(x_i)\right)\cdot \overline{I}_{in}^{(1)}\Big)\\ &\quad \times \frac{\overline{a}_{rest,22}^{(1)}(l_i - x_i)}{\overline{a}_{rest,12}^{(1)}(l_i - x_i)}\,.\end{aligned} \tag{2.1}$$

The resulting form of the criterion is obtained by substituting current $\overline{I}_{rest}$ from Equation (2.1) to basic form of criterial equation:

$$\begin{aligned}&\overline{b}_{i,11}^{(1)}(x_i)\overline{U}_{in}^{(1)} + \overline{b}_{i,12}^{(1)}(x_i)\overline{I}_{in}^{(1)} + \overline{b}_{i,11}^{(2)}(x_I)\overline{U}_{in}^{(2)} + \overline{b}_{i,12}^{(2)}(x_i)\overline{I}_{in}^{(2)}\\ &\quad + \overline{b}_{i,11}^{(0)}(x_i)\overline{U}_{in}^{(0)} + \overline{b}_{i,12}^{(0)}(x_i)\overline{I}_{in}^{(0)} = 3R_f\Bigg(\\ &\left(\overline{b}_{i,21}^{(1)}(x_i)\overline{U}_{in}^{(1)} + \overline{b}_{i,22}^{(1)}(x_i)\overline{I}_{in}^{(1)}\right) - \Big(\overline{b}_{i,11}^{(1)}(x_i)\overline{U}_{in}^{(1)}\\ &\quad + \overline{b}_{i,12}^{(1)}(x_i)\overline{I}_{in}^{(1)}\Big)\frac{\overline{a}_{rest,22}^{(1)}(l_i - x_i)}{\overline{a}_{rest,12}^{(1)}(l_i - x_i)}\Bigg).\end{aligned} \tag{2.2}$$

The equation represents a polynomial of n^{th} order where the unknown variable is fault distance x_i. Since the tested part had been replaced by a cascade connection of two Π-equivalent circuits, the equation represented a polynomial of eighth order with a solution in the form of eight roots $x_{i,1}, \ldots, x_{i,8}$ representing a possible fault distance.

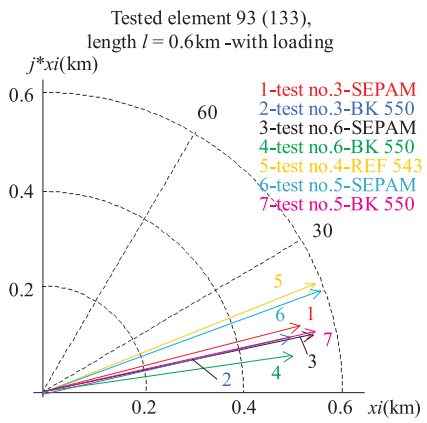

Fig. 2.4. Polynomial roots representation in the complex plane.

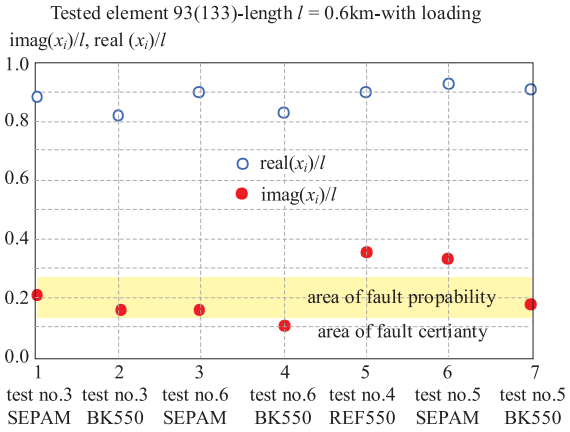

Fig. 2.5. Relative values of real and imaginary parts of polynomial roots.

The roots of the polynomial that are functions of currents $\overline{I}_{in}^{(1)}$, $\overline{I}_{in}^{(2)}$, $\overline{I}_{in}^{(0)}$ and voltages $\overline{U}_{in}^{(1)}$, $\overline{U}_{in}^{(2)}$, $\overline{U}_{in}^{(0)}$ at the input of the tested network element (Equation 2.2) were calculated by means of a procedure for the calculation of polynomial coefficients in Matlab program that uses the Newton method.

Results of Calculations

The crucial criterion for accepting the fact of a fault in the tested part is a real value (or – at least – approximately real value) of some of the roots, obviously only a case where the value is positive can be taken into account. According to [1], one of the possible ways of evaluating the roots of the polynomial is dividing the complex plane into three parts that represent the areas of vectors with defined real and imaginary parts. Then a decision is made whether the fault is, is not or could be in the tested part (see Fig. 2.3).

According to Fig. 2.3, root $x_{i,1}$ or $x_{i,2}$ has a value that corresponds to a possibility of the fault in the i^{th} part of the line, while in case of value $x_{i,3}$ the possibility of the fault in the tested part of the line of length l_i is excluded.

In the first phase of the calculation, a part with a simulated fault was tested. The roots were calculated both for a network model with a simulated load and a no-load model. The results were much better for the model including the load. Values $\overline{U}_m^{(syst)}$ and $\overline{I}_m^{(syst)}$ from all series of measurement for a resistive ground fault obtained from measuring devices were used for testing.

One root with a real part corresponding to the length of the tested part element was found in each step of calculation.

For evaluation of these roots, their representation in the complex plane can be used Fig. 2.4, which can be a little difficult if the roots are close to each other. A better way of representing the results is shown in Fig. 2.5 where there are relative values of real and imaginary parts according to the length of the tested part.

2.3 Sensitivity Analysis

Change in the Length of the Tested Element

Since the fault was simulated at the end of the line element (Fig. 2.6 — part between buses 62 and 94) that was followed by two other line elements, it was possible to extend the tested element (Fig. 2.6 — part between buses 62 and 95). The extension of the tested element led to a significant improvement of the results of tests. The imaginary part of the roots representing a possible fault distance in the tested element is much lower, thus the fault is identified in the element for all presented series of measurement, while at the element length of 0.6 km (results shown in Fig. 2.5) the fault is identified in only five out of seven cases.

Change of Tested Element

The principle of the method lies in sequential testing of elements of the affected line described in the previous part. It is thus supposed that the results corresponding to the identification of the fault apply only to the part where the fault really occurs. That is why it is necessary to verify what results the application of the criterion yields in the non-affected parts of the line and exclude a possibility of false solutions (*ie* in non-affected parts).

For this purpose the remaining two elements of the line behind the point of the fault were tested — between buses 94 and 96 (134 and 136) — and also elements 62-63, 63-64, 64-65 and 51-52 before the point of the fault. The values from all series of measurement and for both network models (with and without load) were used in calculations. The results of the tests can be found in Tab. 2.1.

The position of the tested elements of line V98 is shown in Fig. 2.6. It was intentional to test the element with same or similar electrical distance from the switching station (elements 62-63,63-64, 64-65, 94-95, 95-96) and for comparison also one element at the beginning of line V98

Table 2.1. Test results for selected elements of line V98 (non-affected).

Tested Element	Network Model	Test 3		Test 4	Test 5		Test 6	
		BK 550	SEPAM	REF 543	BK 550	SEPAM	BK 550	SEPAM
94(134) - Buses 94-95	With Load	P	X	X	X	X	P	P
$l = 0.35$ km	Without Load	X	X	X	X	X	X	P
95135) - Buses 95-96	With Load	X	X	X	X	X	X	X
$l = 2.05$ km	Without Load	X	X	X	X	X	X	X
62 – Buses 62-63	With Load	X	X	X	X	X	X	X
$l = 0.2$ km	Without Load	X	X	X	X	X	X	X
63 – Buses 63-64	With Load	X	X	–	–	–	X	X
$l = 0.3$ km	Without Load	X	X	–	–	–	X	X
64 – Buses 64-65	With Load	P	P	–	–	–	P	P
$l = 2$ km	Without Load	C	C	–	–	–	C	C
51 – Buses 51-52	With Load	X	X	–	–	–	X	X
$l = 1.25$ km	Without Load	X	X	–	–	–	X	X
X	Non-Affected							
P	Probability of Fault							
C	Certainty of Fault							

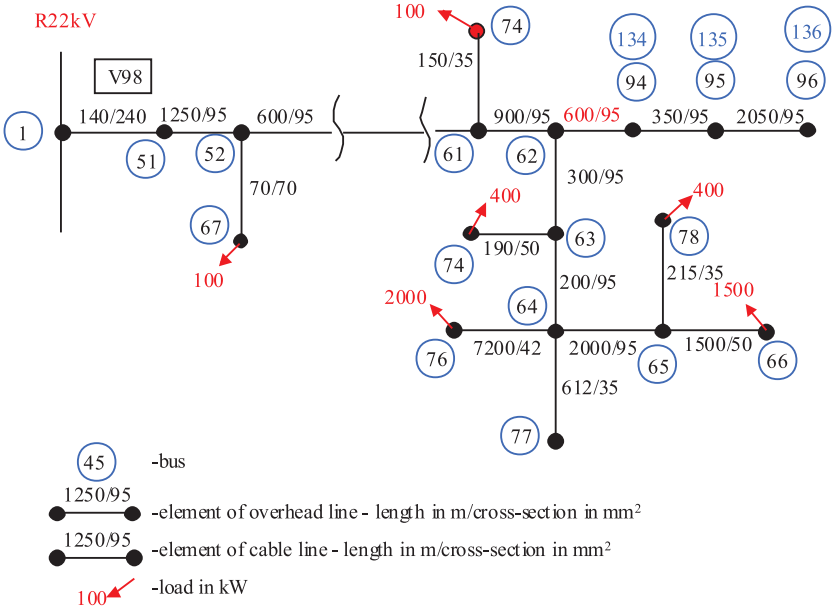

Fig. 2.6. Simplified scheme of line V98 with selected tested elements.

(element 51). The tests of elements 63, 63, 64 and 51 were performed in a smaller network, *ie* only for the values of the third and sixth series of measurement.

It is obvious from the results in Tab. 2.2 that false identification appears in case the transmission elements of the network before and behind the tested element correspond approximately to element 62-93 where the fault was simulated, *ie* in elements 93-94 and 64-65. Assuming that the impedance before the point of the fault for tested elements 62, 63, 64 and 94 with regard to the extension of the network did not change much, it is clear that the most important factor was the remaining part of the network behind the point of the fault.

Change in Fault Resistance

Since the resistance of the fault is not known in advance, it is supposed that this method of ground fault location will always work with an assumed value of fault resistance. It can be chosen on the basis of long-term network analysis and measuring and applied experimentally within a certain range of values that are characteristic for this network. According to [2] the values of fault resistance are somewhere between tens of ohms and hundreds of kiloohms. Contemporary protecting systems of compensated networks are able to find a probable value of resistance at permanent ground fault by means of current injecting to a network bus.

During the analysis of the influence of the value of resistance R_f used in the criterial equation on the values

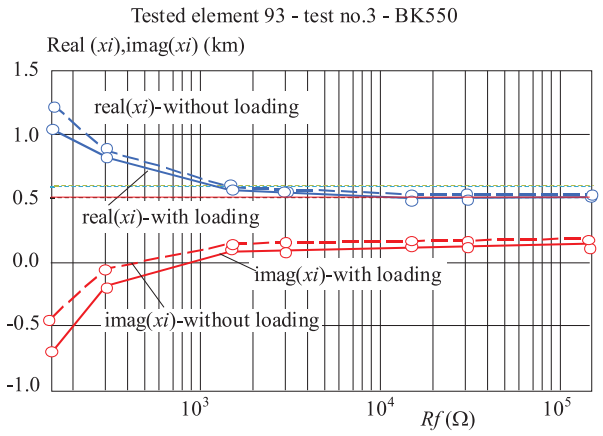

Fig. 2.7. Dependence of the values of the real and imaginary parts of the polynomial roots on fault resistance -- BK 550, the third series of measuring.

of roots (*ie* probable fault distances), the range of R_f between 50 Ω and 150 kΩ was used. The influence on the results of tests is shown in a graphical form as a dependence of the values of the real and imaginary parts of the calculated roots on the resistance, again for two variants with and without load in Fig. 2.7. The figure applies to testing of the element with a simulated fault according to the values from the third series of measurement (the length of the tested element is marked green).

For values of resistance less than 50 Ω, the real parts of roots were of the length of the tested element and the imaginary ones were negative. On the contrary, for values of resistance greater than 2 kΩ, the values of roots remained almost constant, with values approximately equal to those presented in the previous part.

2.4 Conclusions

The results of measurement and calculations during the tests of line elements can be evaluated according to their correspondence with the real situation in the network, especially from the point of view of fault identification in the line element with a simulated fault or false acting in non- affected parts.

From the results presented above, it is clear that the following factors are particularly important for successful identification of faults:

Network Model

A network model as precise as possible need to be used for the location of a simulated fault, it is necessary to model the network including the actual load.

Tested Element Length

The results of tests are better if a longer element is tested where the imaginary part of the calculated probable fault distance is relative smaller. Fault distance calculation proved that the value of the imaginary part for a given point in the network does not change much and is given by the precision of measuring and calculation. Possible testing of a longer line element allows to eliminate the errors of the network model and measuring and thus influences positively the results of tests. However, this requirement limits the selectivity of the method and can be applied only in the case of a convenient network configuration, such as in our situation, where the fault was simulated at the very end of an element of line 93 followed by two elements without branches.

Values Measured in the Switching Station at Ripple-Control Signal Frequency

The results of tests for different variants of measuring differed significantly mainly in the value of the imaginary part of the calculated roots and thus in the successfulness of fault location in the line element with the simulated fault. The overview of the test results in the line element with the simulated fault can be found in Tab. 2.2.

The differences in results show a possible influence of different conditions during various series of measurement (different resistance connected to the point of the fault, different size of the network), but mainly the fact that the successfulness of fault location is strongly influenced by the precision of measurement. The results of the tests corresponded to the precision of instruments — they were better for calculations using the values from BK 550 with a sample frequency much higher then the other two instruments (SEPAM, REF 543).

Values of Fault Resistance Used in the Criterial Equation

It can be conclude from the graphs that the results of testing will not be affected by the value of fault resistance if they are greater than approximately 1 kΩ. This insensitivity to higher fault resistance proves the suitability of the method for the location of fault with high resistance.

According to the obtained results, the location method applied to the element with the simulated fault was successful only in one case, in the other cases the fault was either evaluated as only probable or excluded. If we accept only the results of the tests for the line element with the simulated fault, it can be stated that the method demands relatively high precision. The problem of precision, however, applies not only to measuring but also to the whole process of calculation, from the Fourier transform to the solution of polynomial roots.

The key role in successful fault identification belongs to the faithfulness of the mathematical model of the network. The calculations proved that only after obtaining a corresponding network model verified by the calculation of fault current and voltage, the method can yield usable results.

Table 2.2. The test results in the line element with a simulated fault.

Tests	Network Extent	Fault Resistance	Tested Element			
			93(133) Length $l = 0.6$ km		93+94 (133+134) Length $l = 0.95$ km	
	I_C (A)	R_f (Ω)	Without Load	With Load	Without Load	With Load
3 - BK 550	63	8 000	P	P	C	C
3 - SEPAM			X	P	C	C
4 - REF 543	147		X	X	P	P
5 - BK 550		2 500	X	P	P	C
5 - SEPAM			X	X	P	P
6 - BK 550	63		P	C	C	C
6 - SEPAM			X	P	C	C
X	Non-Affected					
P	Probability of Fault					
C	Certainty of Fault					

Possible Ways of Further Research

The further research should concentrate on the following areas:

- Perform an experiment with a higher number of simulated faults at more points in the network.
- Create a more precise model incorporating the zero-sequence admittance of the network phases. The applied network model was symmetrical and neglected the non-symmetrical nature of the measured network.
- Using the more precise model, verify the sensitivity of the method to the change of the point of the fault in the line element.

Acknowledgements

This paper was made within project KJB2813304 supported by the Grant Agency of the Academy of Science of the Czech Republic.

References

[1] WELFONDER, T. *et al* : Location Strategies and Evaluation of Detection Algorithms for Earth Faults in Compensated MV Distribution Systems, IEEE Transactions on Power Delivery **15** No. 4 (2000), 1121–1128.

[2] HANNINEN, S.—LEHTONEN, M. : Characteristic of Earth Faults in Electrical Distribution Networks with High Impedance Earthing, Electric Power System Research No.44 (1998),155-161.

[3] ORSÁGOVÁ J,—TOMAN P.—HALUZÍK E. : The Method for the Estimation of Earth Fault Location (Metoda pro pravděpodobné určení místa zemního spojení), In ELEKTROENERGETIKA, Stará Lesná, 16–18 September 2000. (in Czech)

[4] LEITLOFF, V.—FEUILLET, R.—GRIFFEL, D. : Detection of Resistive Single-Phase Earth Faults in a Compensated Power-Distribution System, ETEP **7** No. 1 (1997), 65–73.

[5] PROCHÁZKA, K. : Selected problems of Distribution MV Networks Operation (Vybrané problémy provozu distribučních sítí, Příručka pro provozní pracovníky), České Budějovice: Výzkumný stav energetický, 1992. (in Czech)

[6] VALSA, J. : Algorithms for Simulation of Linear and Nonlinear Circuits on PC (Algoritmy pro simulaci lineárních a nelineárních elektronických obvodů na počítači), Brno: Vysoké učení technické v Brně, 1997. Studijní text k vybraným kapitolám postgraduálního doktorandského studia. (in Czech)

[7] POSPÍŠIL, J. *et al* : Algorithms for Simulation of Linear and Nonlinear Circuits on PC (Aplikace nových metod při indikaci zemních spojení v sítích vn), In: Sborník přednášek konference ČK Cired 2001. Tábor 2001, pp. 3/34–3/37. (in Czech)

[8] HANŽLÍK, J.—BÜRGER, P. : Measuring of 22kV Networks Impedance at Frequency 216.6 Hz (Měření impedancí sítí 22 kV na frekvenci 216.6 Hz), In: Sborník přednášek konference ČK Cired 2001. Tábor 2001, pp. 3/38–3/40. (in Czech)

[9] VARGA, L.—ILENIN, S.—LEŠČINSKÝ, P. : Transmission and Distribution of Electrical Energy (Prenos a rozvod elektrickej energie), Mercury-Smékal, Košice, 2003. (in Slovak)

[10] Electrical Energy Distribution (Distribuce elektrické energie), Odborný buletin regionlních energetických společností, květen 2000, č. 27. Jihomoravsk energetika, a.s. (in Czech)

[11] VARGA, L.—LEŠČINSKÝ, P.—BEŇA, Ľ. : The Complex Solution of Overhead Transmission Lines Mechanics in a Plain, Analele Universitatii Din Oradea, Fascicola Elektrotechnika, mai 2001 pp. 302–323.

[12] CHLADNÝ, V.—HVIZDOŠ, M.—MEŠTER, M. : Fault Location in Overhead Lines (Identifikácia miesta poruchy na vonkajších vedeniach), In: Aktuálne problémy elektroenergetiky a techniky vysokých napätí, Ferrost a.s., Košice, Slovakia, 2000, pp. 17–22.

Received 30 September 2004

Petr Toman (Ing, PhD) graduated in power current electrical engineering and electro-power engineering from the Faculty of Electrical Engineering and Computer Science, Brno University of Technology in 1998. In 2001 he graduated in company management and economics from the Faculty of Business and Management. He received the PhD degree in 2002 from the Faculty of Electrical Engineering and Communication.

He has worked at the Department of Electrical Power Engineering since 2001. He specializes in fault protection and fault location on HV lines, power systems operation and control. He is a member of the IEEE.

Jaroslava Orságová (Ing, PhD) graduated from the Faculty of Electrical Engineering of Brno University of Technology in 1987. She received the PhD degree in 2004 from the Faculty of Electrical Engineering and Communication.

She has worked at the Department of Electrical Power Engineering since 1996. Her teaching and research activities cover the field of power plants and nuclear power plants and switchgears.